APPLICATIONS FOR INFRARED IMAGING EQUIPMENT IN PHOTOVOLTAIC CELL, MODULE, AND SYSTEM TESTING

D. L. King, J. A. Kratochvil, and M. A. Quintana
Sandia National Laboratories, Albuquerque, NM, 87185

T. J. McMahon
National Renewable Energy Laboratory, Golden, CO, 80401

ABSTRACT

Anomalous temperature distributions are often an indication of atypical behavior in a device under investigation. Portable infrared (IR) imaging systems (cameras) now provide a convenient method for measuring both absolute and relative temperature distributions on small and large components with a high degree of temperature and spatial resolution. This diagnostic tool can be applied during the development, production, monitoring, and repair of photovoltaic cells, modules, and systems. Planar objects with nearly uniform material composition are ideally suited for analysis using IR imaging. This paper illustrates investigations of localized shunting in cells, resistive solder bonds in field-aged modules, module bypass diode functionality, reverse-bias (hot spot) heating in modules, temperature distributions in flat-plate and concentrator modules, batteries during charging, and electronic component temperature in power processing equipment.

INTRODUCTION

All materials emit infrared (IR) radiation over a range of wavelengths that depends on the temperature of the material. The infrared heat emitted by a material is quantified by the Stefan-Boltzmann law, and the spectral distribution of the emitted energy is expressed by Planck's distribution [1]. For the components of interest in photovoltaic systems (cells, modules, arrays, bypass diodes, wiring terminals, batteries, etc.) the temperature range of most interest is perhaps 0 °C to 150 °C. For example, a typical PV module at 50 °C emits heat primarily in the wavelength range from 3 μm to 20 μm, with peak emittance at about 9 μm. Commercially available infrared cameras can be purchased with lenses and detectors customized for operation with different wavelengths of light. A digitized IR image of an object can then be directly related to the temperature distribution across the object.

The IR camera used for the analyses presented in this paper was a FLIR Prism DS camera with a detector composed of a 320 x 244 IR-CCD array of platinum silicide (PtSi) elements. The detector is mechanically cooled with a Stirling engine. The camera and lens combination had IR sensitivity in the 3.6 to 5.0 μm range. Lenses available for this camera provided both close-up imaging of small solar cells or normal-imaging of large objects such as PV arrays. Resolution of temperature differences on the order of 0.1 °C and spatial resolution of less than 0.01 mm^2 were achieved. Sophisticated software for data interpretation, charting, and analysis is also available for the FLIR system. The primary disadvantage of these systems is cost; camera, multiple lenses, software, and other miscellaneous components may cost about $50,000. However, IR technology is rapidly evolving, and for many of the applications illustrated in this paper, IR imagers of much lower cost may provide valuable qualitative information regarding temperature distributions.

LOCALIZED SHUNTING IN CELLS

A problem often encountered during cell manufacturing, and sometimes as a result of field aging, is a localized shunting path within a solar cell. During manufacturing this might occur as the result of impurities on wafers during junction diffusion, an ineffective edge isolation process, non-uniform deposition of thin-film cells, or incomplete scribe lines in thin-film modules. Field aging may result in moisture intrusion into modules with resulting corrosion leading to shunting failures, particularly in thin-film modules. Physically locating shunt paths in a solar cell makes it possible for researchers to focus their diagnostic investigation on the affected spots. IR imaging can be used to locate these spots. The test procedure required uses a dc power supply to force current through the cell in a reverse-biased condition. In reverse bias and without illumination, current flows preferentially through any available shunt paths. This current flow through locations with low shunt resistance leads to localized heating. Figures 1 and 2 show the temperature distributions for two different solar cells using digitized IR images recorded within a few seconds of introducing reverse-biased current flow through the cells. In locating shunts, it is desirable to record the images quickly after current flow is introduced, otherwise lateral heat transfer in the cell causes the temperature to "bloom" masking the exact location of the shunt. Figure 3 shows an IR image of a small area on an interdigitated back-contact emitter-wrap-through (EWT) cell. The lines are metal contact fingers and the small spots are 70-μm diameter (0.004 mm^2) holes through the cell, indicating the fine resolution of the IR camera.

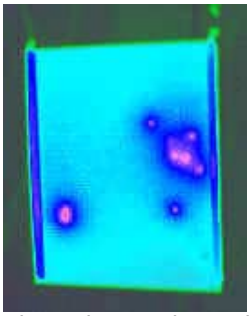

Fig. 1. Localized shunts in experimental back-contact, 40 cm^2, emitter-wrap-through silicon cell. 20≤ T ≤39 °C.

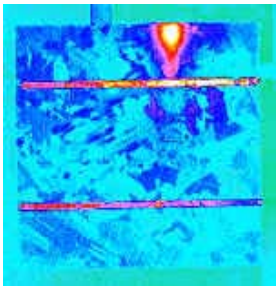

Fig. 2. Localized shunt due to inadequate edge isolation during production of 100-cm^2 mc-Si cell. 20≤ T ≤40 °C.

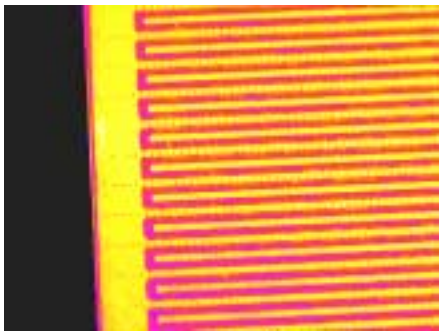

Fig. 3. Close-up IR image of interdigitated metal fingers on experimental EWT cell. Small dots are 0.004 mm^2 holes through the cell. 26≤ T ≤39 °C.

IR IMAGING THROUGH GLASS SUPERSTRATES

Often infrared imaging must be done with the cell material encapsulated behind glass. Lateral heat spreading by the glass may affect the ability of the IR camera to detect shunt paths or resistive elements, depending on the situation. Previous work describes efforts to increase the sensitivity of IR imaging through frame averaging, cell modulation, or pulsed lock-in techniques [2, 3]. This issue of lateral heat spreading and dissipation was investigated using a sample with a CIS thin-film cell deposited on a 2-mm thick glass substrate. The cell sample was forward biased to image uniform heating due to recombination current and distributed series resistance. Reverse bias was used to image two localized point-shunt paths on the sample caused by defects in the cell isolation scribe. By recording IR images of both the glass-side and the cell-side of the sample, the effect of the glass and the limitation of the camera in detecting small point-shunts through a glass superstrate was demonstrated. Figure 4 illustrates "line scans" or temperature profiles generated from a digitized IR image of the CIS cell sample. The profile with the sharp peaks was imaged by viewing the CIS surface directly, with thermal emissivity assumed to be e=0.7. The smooth temperature profile was recorded by viewing through the 2-mm thick glass (e = 1). Each peak is several digitized pixels in size. For point-shunts of the size shown in Fig. 4, lateral heat spreading in the glass resulted in the IR camera not being able to detect the sharp temperature rise present.

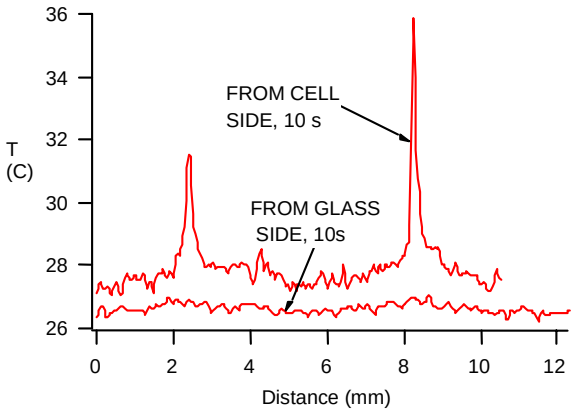

Fig. 4. Temperature profile through point shunts (defects) in CIS cell from IR images recorded of both the cell surface and through the glass substrate, recorded 10 s after -1.1 V reverse bias with 6.9 mA current was applied.

Figure 5 shows temperature profiles for the same CIS cell sample but with the sample in a forward biased condition. These temperature profiles were the same as observed when viewing the cell material directly, except they were free of large fluctuations from grid lines and isolation scribes. For this larger feature (about 4-mm in width), there was no loss in detectability of desired thermal characteristics by viewing through the glass.

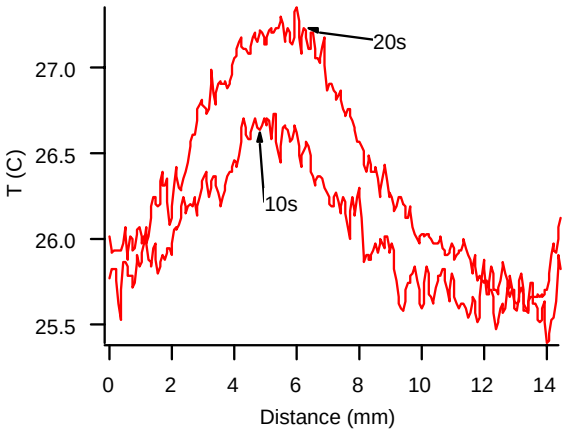

Fig. 5. Temperature profile of CIS cell sample in forward bias (+1.0V) with 42 mA current flow for 10 s and 20 s.

A heat-balance analysis of the case shown in Figure 5 provided an estimate of the temperature rise rate and an assessment of the influence of lateral heat spreading in the glass. For the CIS sample, the rate that temperature increased, dT/dt, was 0.06 °C/s. Using the heat capacity of the glass (0.8 J/°C/gm), thermal conductivity of glass (0.4 W/cm/°C), and the volume of glass (0.064 cm^3) in contact with the cell sample, an estimate of the expected temperature rise rate was determined without the influence of lateral heat spreading in the glass. Without lateral thermal conduction to adjacent glass, and without radiative or convective heat losses, the calculated rate that temperature should rise is about 10 times higher than actually observed. Nonetheless, for localized heat sources on the order of 4-mm in size, IR imaging through 2-mm glass superstrates is as effective as viewing the cell sample directly. Similar analyses indicated that for a localized heat source, about 10 mW of heat dissipation was required to raise the local temperature in a glass/cell laminate by 4 °C.

RESISTIVE SOLDER BONDS IN MODULES

All current flowing through a module must flow through the cell interconnect ribbons and then through discrete solder bonds into the solar cell's metallization. Resistive or failed solder bonds resulting from field aging cause the current to flow through a reduced number of solder bonds. This increased current density causes localized heating at the functional solder bond locations. IR imaging can be used to analyze the temperature distribution in new and field-aged modules by forcing current through the module with a dc power supply. Figure 6 illustrates the temperature distribution in a field-aged (5 years) module with a current about 1.5 times the one-sun short-circuit current flowing through the module. The image illustrates a situation where solder bonds have failed, resulting in high current densities (hot spots) in the remaining solder bonds on two different cells. Similar images for new modules exhibit a relatively uniform temperature distribution across all cells. Again, the IR images facilitate the diagnostic evaluation of failure mechanisms in PV modules.

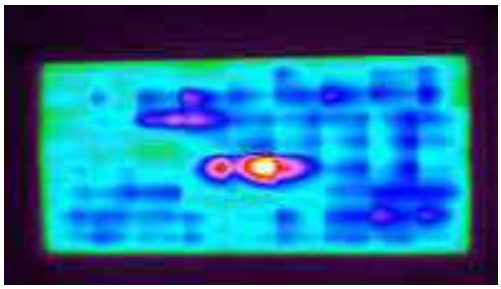

Fig. 6. IR image of 36-cell silicon module with defective solder bonds after 5 years in the field; forward biased with 5 A current flow. 36≤ T ≤76 °C

REVERSE-BIAS HEATING IN MODULES

When modules with series-connected cells are short circuited, individual cells in the module can heat up significantly. This is a common occurrence in silicon modules even without manufacturing defects or field-aging problems. Production variation results in individual cells having several percent difference in their short-circuit currents (I_{sc}). When the module is short-circuited under outdoor solar illumination, the cells with the lowest I_{sc} are forced to operate in a reverse-biased condition, and as a result, dissipate energy within the cells and heat up. As a rule-of-thumb, about 3W of power continuously dissipated in a 100-cm^2 cell will raise its temperature by 10 °C relative to other cells. Although not typically harmful to the module, this phenomenon can be used in conjunction with IR imaging as a field diagnostic method. Figure 7 illustrates the patchwork temperature distribution in an operating array of modules where an array wiring problem inadvertently resulted in an entire series-string of modules being short circuited. The "hot spot heating" procedure associated with module qualification testing [4] introduces the same reverse-bias heating phenomenon by intentionally shading individual cells in a module, a situation for which IR imaging would also be beneficial.

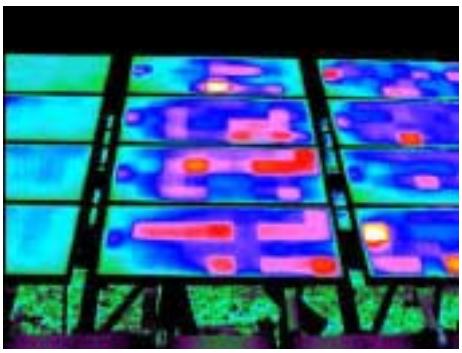

Fig. 7. IR image of array in operation with a string of modules inadvertently short-circuited. Patchwork heating is typical for silicon modules. 52≤ T ≤80 °C

BYPASS DIODE FUNCTIONALITY

Commercial PV modules are often equipped with bypass diodes to partially compensate for performance losses due to module shading and to minimize the reverse-bias heating phenomenon previously mentioned. IR imaging can be used to perform a quick functionality test of bypass diodes either during the manufacturing process or as a subsequent diagnostic test. Figure 8 illustrates the procedure for a thin-film module equipped with bypass diodes around each of 22 cells. In this case, the bypass diodes were located under the aluminum module frame to aid in heat dissipation. A dc power supply was used to supply current to the module terminals, with the cells in reverse bias, resulting in current flow through the forward-biased bypass diodes but not the cells. A temperature rise in the bypass diodes indicated they were functioning correctly.

MODULE TEMPERATURE DISTRIBUTIONS

Module mounting configurations, wind speed, and wind direction can introduce significant spatial variation in outdoor module operating temperatures. For instance, directly mounting modules to the roof of a building can

result in not only increased temperatures but dramatic temperature distributions, as shown in Figure 9.

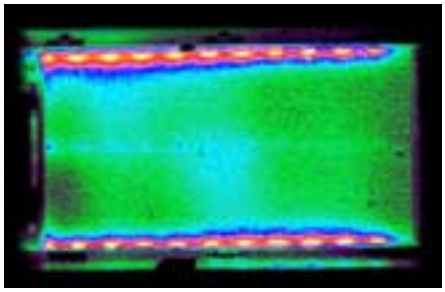

Fig. 8. With module in reverse bias, bypass diode functionality verified by passing current through forward-biased bypass diodes. 23≤ T ≤31 °C

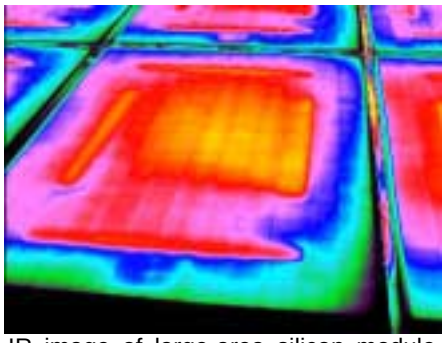

Fig. 9. IR image of large-area silicon module in array mounted on a horizontal roof. Patterns in temperature distribution introduced by polymer stand-offs used to support the modules. 60≤ T ≤72 °C

BATTERIES AND OTHER BOS COMPONENTS

Many analogies between arrays of PV modules and battery banks used for energy storage can be illustrated and employed using IR imaging. Batteries operate in the equivalent of forward and reverse bias conditions, depending on whether the batteries are supplying power (current) or are being charged by current supplied from a PV array. When current is flowing, resistive battery terminals dissipate unnecessary power and consequently appear abnormally hot when viewed with an IR camera. During the charging process, battery banks dissipate heat internally producing a stratification of temperature in the individual cells of the battery bank, as shown in Figure 10. In addition, as battery banks age, individual cells degrade at different rates resulting in cell to cell mismatch and non-uniform temperatures during charging. In all these situations, IR imaging provides a quick method to diagnose the health of a battery bank.

Similarly, resistive wiring terminations in array junction boxes, malfunctioning array blocking diodes, and abnormally hot components in inverters or other power processing equipment can be identified using IR imaging. Figure 11 illustrates the temperature distributions evident on components inside an inverter during normal operation.

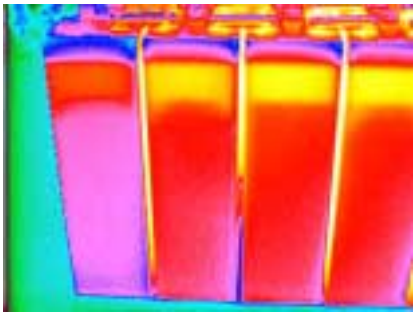

Fig. 10. Four individual cells in a large battery bank during the charging process. Temperature stratification in electrolyte, and cooler end cell due to larger area exposed to ambient air. 25≤ T ≤38 °C

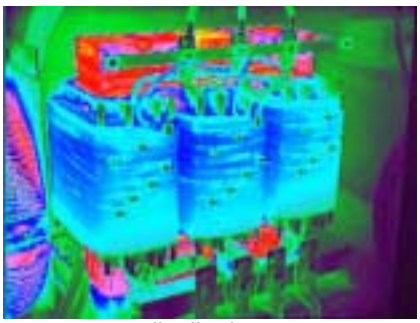

Fig. 11. Temperature distributions on components inside PV system inverter during operation. 28≤ T ≤45 °C

CONCLUSIONS

The ability to directly view temperature distributions in PV system components (cells, modules, arrays, batteries, and power processing equipment) provides a valuable diagnostic tool that is applicable during the development, production, monitoring, and repair of all photovoltaic system components.

AKNOWLEDGEMENTS

The authors would like to acknowledge valuable discussions regarding localized shunts in solar cells with James Gee and David Smith from Sandia. *[Work supported by the U. S. Department of Energy under contracts DE-ACO4-94AL85000 (Sandia) and DE-AC36-83CH10093 (NREL). Visit our websites at www.sandia.gov/pv and www.nrel.gov/ncpv.*]

REFERENCES

[1] R. Siegel and J. Howell, Thermal Radiation Heat Transfer, McGraw-Hill Book Company, 1972.
[2] A. Kaminski, et al., "Infrared characterization of hot spots in solar cells with high precision due to signal treatment processing," *Solar Energy Materials and Solar Cells* **51**, 1998 pp. 233-242.
[3] M. Langenkamp, et al., "Microscopic Localization and Analysis of Leakage Currents in Thin Film Silicon Solar Cells," *16th European PVSEC*, 2000.
[4] IEEE Standard 1262. "Recommended Practice for Qualification of Photovoltaic (PV) Modules."